Pol. J. Environ. Stud. Vol. XX, No. X (XXXX), 1-13
DOI: *10.15244/pjoes/216344* ONLINE PUBLICATION DATE: 2026-02-27

Original Research

Enhanced Nitrogen Removal Performance of Anammox Process for Saline Wastewater Treatment via Sheep Manure Biochar Addition

Jiao Chen[1, 2, 3°], Fangying Liu[1], Siyu Yan[1], Senmiao Niu[1], Zhipeng Zhang[3], Yixin Lu[1, 2, 3*]

[1]School of Materials and Environmental Engineering, Chengdu Technological University, Chengdu 611730, China
[2]Sichuan Provincial Engineering Research Center of Livestock Manure Treatment and Recycling, Sichuan Normal University, Chengdu 610068, China
[3]Engineering & Technology Center of Groundwater Pollution Control for Environmental Protection in Sichuan, Sichuan Geological Environment Survey and Research, Chengdu 610081, China

Received: 08 September 2025
Accepted: 02 January 2026

Abstract

Anaerobic ammonia oxidation (anammox) granular sludge was used to treat simulated saline wastewater, and the effect and mechanism of sheep manure biochar (SMB) addition on the enhancement of nitrogen removal performance when the process was inhibited by high salinity were investigated. The results showed that the nitrogen removal effect deteriorated with increasing salinity as influent salinity reached 2% and above. With a one-time addition of 5 g/L SMB, the reactors inhibited by 2% and 3% influent salinity were able to recover their nitrogen removal performance after 18 and 34 days of operation, respectively, and the total nitrogen (TN) removal efficiencies were stabilized at 90% or more. At an influent salinity of 4%, the TN removal efficiency recovered to over 70% after dosing 5 g/L of SMB twice and running for 43 days. For an influent salinity of 5%, the relief of salinity inhibition by increasing the amount and frequency of SMB dosing was not significant. With its abundant pore structure and rich surface functional groups, SMB created favorable conditions for promoting microbial attachment and growth, extracellular polymeric substances secretion, sludge-specific anammox activity, and electron transfer activity. The moderate dosing of SMB can effectively alleviate the inhibitory effect of high salinity on nitrogen removal and provide a useful strategy for the efficient application of the anammox process in saline wastewater treatment.

Keywords: saline wastewater, anammox, sheep manure biochar, nitrogen removal

*e-mail: yxlu61@163.com
Tel.: +86-159-286-28507
Fax: +86-028-879-92337
°ORCID iD: 0009-0002-4083-4627

Introduction

Anaerobic ammonia oxidation (anammox), as the most promising type of technology for the removal of nitrogenous pollutants from wastewater, enables the simultaneous and efficient removal of ammonia nitrogen (NH_4^+-N) and nitrite nitrogen (NO_2^--N) without the supply of an additional organic carbon source [1]. Compared with the traditional biological nitrogen removal technology, the anammox process features lower energy consumption, less residual sludge production, and higher product cleanliness, and enables the nitrogen removal of nitrogenous wastewater with a low carbon/nitrogen ratio and high concentration that cannot be treated by the traditional process and possesses significant energy-saving and consumption-reducing characteristics [2]. Recently, the anammox process has been applied to treat various types of nitrogenous wastewater, such as swine digested wastewater [3], landfill leachate [4], secondary wastewater [5], mainstream municipal wastewater [6], etc., and has achieved a considerable nitrogen removal effect. However, anammox bacteria (AnAOB), as the core functional bacteria of the process, are autotrophic microorganisms with slow growth and high environmental sensitivity, resulting in a long cell multiplication time and poor holding capacity [7]. When environmental conditions change, their resistance and adaptability may be weakened, ultimately affecting the nitrogen removal performance of the anammox process.

Among the various influencing factors, salinity is considered to be a common factor that significantly affects microorganisms in wastewater treatment plants [8]. Large quantities of saline effluents are generated during industrial production, food processing, and seawater reuse, which converge or infiltrate into the urban sewage network, increasing the salinity of the mainstream wastewater. The change in osmotic pressure caused by the increase in salinity reduces the metabolic activity of microorganisms and produces a coercive effect, which makes it difficult to treat saline wastewater biologically [9]. To address this problem, existing studies have explored a series of methods to improve the treatment performance of bioreactors in a high-salt background, such as inoculation of salt-tolerant sludge [10], supplementation of potassium ions [11], application of low-voltage stimulation [12], and dosing of cell-permeable protectants [13]. These methods have certain feasibility, but with different degrees of operation complexity, time-consuming, poor stability, high cost, and other drawbacks. When treating saline wastewater, the nitrogen removal performance and bacterial activity of the anammox process are similarly affected by salinity [14]. Therefore, exploring strategies to improve nitrogen removal performance when inhibited by salinity is of great practical significance for the application and extension of the anammox process in saline wastewater purification.

Biochar, as a new type of functional material with low cost, good performance, and environmental friendliness, is gaining popularity in wastewater treatment [15]. In recent years, some studies have been reported on the application of biochar in the anammox process, where the combination of biochar and the anammox process can shorten the start-up time of the bioreactor, improve the nitrogen removal performance, and mitigate pollutant inhibition [16]. In the treatment of saline wastewater, biochar has been recognized for its potential to mitigate salt stress, promote microbial activity, and enhance system stability due to its unique physicochemical properties. Yang et al. [17] demonstrated that adding microalgae-derived biochar to a microalgae-bacterial granular sludge system treating 0.3% saline aquaculture wastewater significantly improved granular sludge stability and system resilience, elevating the modified system's ammonia nitrogen removal rate to 87.1%. Zhao et al. [18] incorporated biochar prepared from Cyperus alternifolius and immobilized with halotolerant aerobic denitrifying bacteria into the substrate during constructed wetland treatment of saline wastewater. Under low C/N ratios, this approach achieved approximately 70% removal rates for NO_3^--N and TN. These studies showed that biochar enhanced nitrogen removal in biological treatment systems by providing microbial attachment sites, promoting extracellular polymeric substances (EPS) secretion, improving sludge settling properties, or augmenting electron transfer efficiency [19]. Different types of biochar showed significant variations in effectiveness when applied to wastewater treatment, making the exploration of efficient raw materials for biochar production critically important. As a major livestock-raising nation, China generates over 200 million tons of sheep manure annually. Except for a small portion used for composting, most is stored in open piles, posing both pollution risks and representing a waste of carbon resources. High-value utilization pathways are urgently needed. Previous studies have reported the successful preparation of sheep manure biochar (SMB) and its application in removing pollutants from various wastewater sources. Its porous framework offers ideal attachment sites for microbial communities, and its rich functional group structure facilitates electron transfer or EPS induction under salinity stress [20, 21]. It is thus theoretically, environmentally, and economically feasible to alleviate salinity inhibition via SMB addition. However, the application of SMB to enhance the nitrogen removal performance of saline wastewater treated by the anammox process has rarely been reported, and its practical feasibility and enhancement mechanism are not yet clear.

In view of this, this study adopted the anammox process to treat simulated saline wastewater, examined its nitrogen removal performance as affected by influent salinity, and attempted to recover it via the addition of laboratory-produced SMB. By investigating the effects of SMB addition on the conversion of nitrogen pollutants

and sludge properties, as well as the structural changes in SMB and the microflora, the feasibility and mechanism of SMB application in enhancing the nitrogen removal performance of the anammox process were explored, to provide scientific insights and technical references for the application of anammox synergized with biochar in treating saline wastewater.

Materials and Methods

Experimental Setup and Operation

The anammox process was operated within anaerobic sequencing batch reactors (ASBRs). The reactor was 2000 mL in size, made of plexiglass material, with an inlet pipe at the bottom, an outlet and sludge discharge ports on the sidewalls, an exhaust port at the top, an internal stirrer, and a black plastic film wrapped around the perimeter. In each reactor, 300 mL of anammox granular sludge, 200 mL of deionized water, and 1000 mL of simulated wastewater were added, and the dissolved oxygen concentration of the wastewater was reduced to less than 0.5 mg/L by introducing nitrogen gas. The process took 12 h for each cycle, comprising 15 min of water intake, 10 h of reaction, 30 min of settling, 15 min of drainage, and 1 h of standstill, with a rotational speed of 160 r/min and a reaction temperature of 35±1ºC.

Influent and Inoculated Sludge

The nitrogen pollutants in the simulated saline wastewater were 100 mg/L of NH_4^+-N and 132 mg/L of NO_2^--N, which were supplied by adding NH_4Cl and $NaNO_2$, respectively. Additionally, 500 mg/L of $KHCO_3$, 10 mg/L of KH_2PO_4, 5.6 mg/L of $CaCl_2$, and 300 mg/L of $MgSO_4 \cdot 7H_2O$ were added to the influent, as well as 1 mL each of the trace element nutrient solution I and II per 10 L of influent. The specific compositions and amounts of the nutrient solutions were described in the literature [22]. The salinity in the influent was replenished by adding NaCl. The stable anammox granular sludge in the laboratory was employed as the inoculated sludge, with a mass concentration of about 9.5 g/L. The sludge was brick-red in color, with a well-defined granularity, and had good nitrogen removal performance for common non-saline wastewater. The granular sludge was rinsed three times with 0.1 mol/L of phosphate buffer to minimize the interference of residual pollutants on the sludge with the accuracy of the subsequent experiments, and then screened out the part with a particle size larger than 1 mm to be added into the ASBRs.

Preparation of SMB

SMB was prepared by the classical oxygen-limited pyrolysis method. The temperature gradient was 9.5ºC/min, and the pyrolysis temperature was 400ºC for 2.5 h. After cooling, 20 mL of 1.5 mol/L NaOH solution was added to each 1 g of pyrolysis product and shaken at room temperature for 1 h. This process was designed to remove soluble ash and tar remaining after pyrolysis of sheep manure feedstock, preventing their entry into ASBRs and causing severe pH fluctuations and additional salinity elevation. Simultaneously, it enabled pore unblocking and exposure of more functional groups via saponification of tar and stripping of ash layers, thereby facilitating subsequent substrate adsorption, microbial colonization, and electron transfer [23]. After shaking, the mixture was rinsed several times with deionized water for 3~5 min each time until the filtrate pH stabilized around 7.5 and solid-liquid separation occurred rapidly. The solid was filtered under vacuum, dried at 55ºC to constant weight, and passed through a 100-mesh sieve to obtain particles smaller than 0.15 mm, yielding the SMB required for the experiment.

Experimental Scheme

Eight groups of ASBRs were set up, numbered as A_0, $A_{0.2}$, $A_{0.5}$, A_1, A_2, A_3, A_4, A_5 in that order. The single-cycle influent and effluent volumes were 1000 mL. Reactor A_0 served as the blank control without any NaCl addition, while reactors $A_{0.2}$, $A_{0.5}$, A_1, A_2, A_3, A_4, and A_5 received NaCl at 2, 5, 10, 20, 30, 40, and 50 g/L, yielding influent salinities of 0.2%, 0.5%, 1%, 2%, 3%, 4%, and 5%, respectively. The nitrogen removal performance under different salinity impacts was investigated, and the ASBRs (A_2, A_3, A_4, and A_5) that suffered from significant inhibition were selected. Appropriate amounts of SMB were dosed and observed to recover the nitrogen removal performance of the anammox process, to explore the feasible SMB addition strategy to alleviate the inhibition of salinity. To facilitate the analysis, the operating phases were divided according to the nitrogen removal under different SMB dosages and addition frequencies. Specifically, the operation of reactors A_2 and A_3 was divided into three phases, with phase II receiving an SMB dosage of 5 g/L, while phases I and III received no additional SMB. The operation of reactors A_4 and A_5 was divided into four phases, with phase II receiving SMB dosages of 5 g/L and 10 g/L, respectively, with phase III at 5 g/L, and no additional SMB dosing in phases I and IV. The determination of SMB dosage and addition frequency was based on preliminary experiments. A scaled-down reaction environment was established in a series of 200 mL serum bottles, with SMB dosage gradients set at 1, 2, 5, 10, and 15 g/L. After a period of operation, it was observed that under relatively low salinity conditions, nitrogen removal efficiency peaked at an SMB dosage of 5 g/L. Conversely, under relatively high salinity conditions, either increasing the SMB dosage to 10 g/L or doubling the dosing frequency was required.

Analytical Methods

The test methods for the concentration of nitrogen pollutants in wastewater were referred to in the Analytical Methods for Water and Wastewater Monitoring (Fourth Edition). Influent and effluent nitrogen concentrations were denoted as $\rho(NH_4^+\text{-N})_{inf.}$, $\rho(NO_2^-\text{-N})_{inf.}$, $\rho(TN)_{inf.}$ and $\rho(NH_4^+\text{-N})_{eff.}$, $\rho(NO_2^-\text{-N})_{eff.}$, $\rho(NO_3^-\text{-N})_{eff.}$, $\rho(TN)_{eff.}$, respectively. The removal efficiencies of NH_4^+-N, NO_2^--N, and TN were denoted by $\eta(NH_4^+\text{-N})$, $\eta(NO_2^-\text{-N})$, and $\eta(TN)$. Volumetric nitrogen removal loading (VNRL) was calculated based on the removal of nitrogen pollutants per unit volume of the reactor. The values of stoichiometric ratios $\Delta NO_2^-\text{-N}/\Delta NH_4^+\text{-N}$ and $\Delta NO_3^-\text{-N}/\Delta NH_4^+\text{-N}$ were calculated based on NO_2^--N consumption (ΔNO_2^--N), NH_4^+-N consumption (ΔNH_4^+-N), and NO_3^--N production (ΔNO_3^--N).

The content of EPS in sludge was calculated as the sum of the concentration of protein (PN) and polysaccharide (PS). PN and PS were analyzed by the Kohmas bright blue method and the sulfuric acid-phenol colorimetric method. The analysis of specific anammox activity (SAA) was calculated by the serum bottle method, based on the change curve of the mass concentration of the substrate. The surface morphology characterization of SMB was performed by the SEM method, the analysis of specific surface area (SSA), total pore volume (TPV), and average pore diameter (ADP) was performed by the BET method, and the analysis of surface functional groups was performed by the FTIR method. Microbiome structure analysis was performed using 16S rRNA high-throughput sequencing.

Results and Discussion

Impact of Salinity on Nitrogen Removal

The conversion of nitrogen pollutants in wastewater by ASBRs under different influent salinities is shown in Fig. 1. For the reactor $A_{0,}$ which was not impacted by salinity, the concentrations of NH_4^+-N, NO_2^--N, and TN in the effluent were 2.6, 0.8, and 22.1 mg/L, respectively, corresponding to the removal efficiencies of 97.4%, 99.4%, and 90.5%, respectively, and the anammox process showed a good nitrogen removal effect. When the influent salinity increased, the nitrogen concentration in the effluent of reactors $A_{0.2}$, $A_{0.5}$, and A_1 did not increase, and their removal efficiencies were improved instead. However, the nitrogen concentration in the effluent of reactor A_2 appeared to increase significantly, and the values of $\eta(NH_4^+\text{-N})$, $\eta(NO_2^-\text{-N})$, and $\eta(TN)$ decreased by 15%, 16.3%, and 16.3%, respectively, compared with reactor A_0. Afterwards, as the influent salinity continued to increase, the concentrations of NH_4^+-N, NO_2^--N, and TN in the effluent of reactors A_3, A_4, and A_5 continued to increase, and the corresponding removal efficiencies continued to decrease. When the influent salinity reached 5%, the nitrogen removal performance

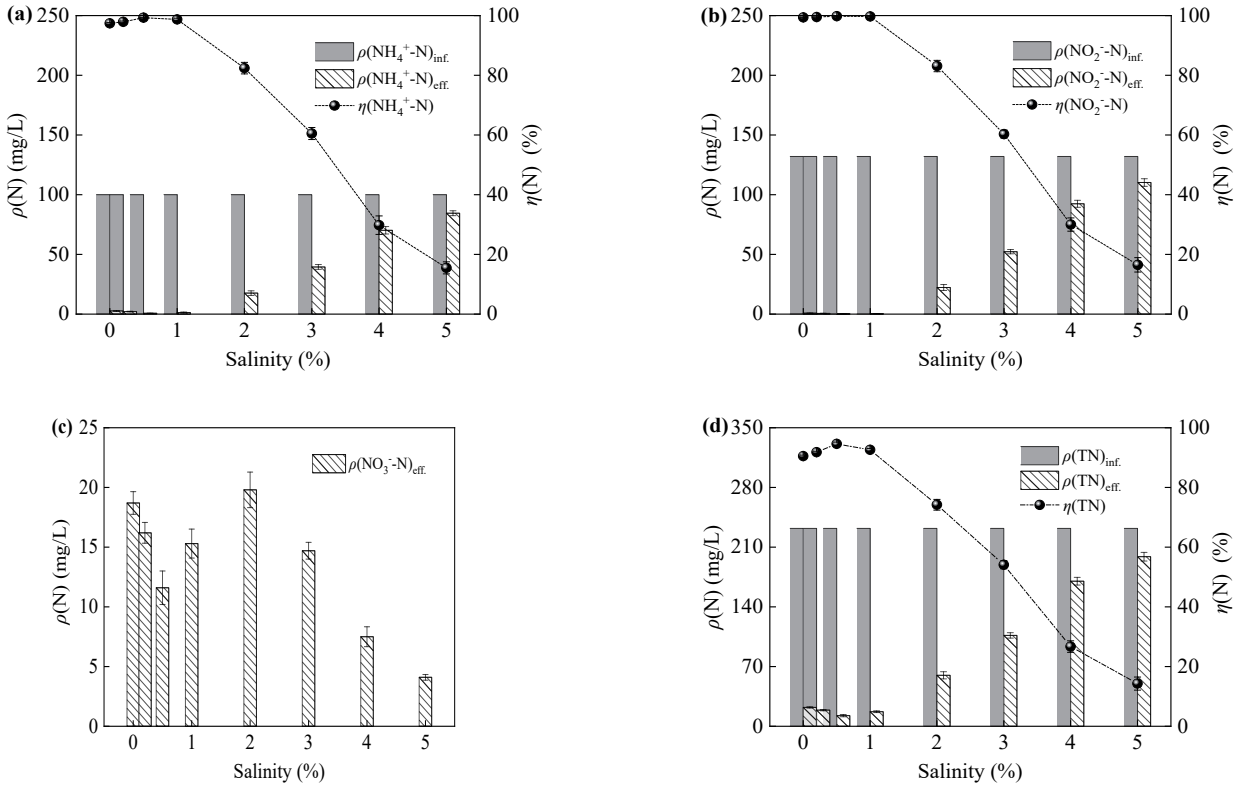

Fig. 1. a) Conversion of NH_4^+-N, b) NO_2^--N, c) NO_3^--N, d) and TN at different salinities.

of reactor A_5 declined sharply, with η(TN) decreasing by 76.2% compared with reactor A_0.

It can be seen that the removal of nitrogen from wastewater by ASBRs was favored when the range of influent salinity was 0.2% to 1%. The proper salinity in water stimulated the stress response of nitrogen-removing bacteria, which could help them to adapt to the environmental changes and improve their metabolic activity, leading to the improvement of nitrogen conversion efficiency [24]. However, when the influent salinity increased to 2%~5%, it negatively impacted the anammox performance. It could lead to excessive osmotic stress, inhibit cellular enzyme activity, damage cellular structure, reduce the metabolic activity of the bacterial flora, or even lead to their death, which in turn hinders the effective conversion of nitrogen [25]. Therefore, when the influent salinity was 2% to 5%, regulatory measures were required to alleviate the salt inhibition to maintain the normal and stable operation of the nitrogen removal process in the ASBRs.

Impact of SMB Addition on Nitrogen Removal

Conversion of Nitrogen Pollutants

Fig. 2 shows the conversion of nitrogen pollutants in wastewater by reactors A_2~A_5 after the addition of SMB. As seen in Fig. 2a), reactor A_2 had a high nitrogen concentration in the effluent in phase I, and the discharge was poor. After the addition of SMB, the effluent concentration of nitrogen pollutants in phase II gradually decreased except for the NO_3^--N concentration. After 18 days of operation, all nitrogen removal efficiencies exceeded 90%. After entering the stabilized stage III, the mean values of $\eta(NH_4^+\text{-N})$, $\eta(NO_2^-\text{-N})$, and η(TN) reached 97.5%, 99.7%, and 91.8%, respectively, which were 15.1%, 16.8%, and 17.6% higher than those in phase I. According to Fig. 2b), the nitrogen concentration in the effluent of reactor A_3 in phase I was higher than that of reactor A_2, and the salinity stress was heavier. After adding SMB, the nitrogen concentration in the effluent in phase II showed a decreasing trend, but this trend was slower than that of reactor A_2, and the NO_3^--N concentration in the effluent still had not changed significantly. After 34 days of operation, the effluent stabilized and entered phase III, and the mean values of $\eta(NH_4^+\text{-N})$, $\eta(NO_2^-\text{-N})$, and η(TN) rebounded to 96.1%, 98.2%, and 90.3%, respectively, which were 36.6%, 38.8%, and 37.6% higher than those in phase I. It was thus shown that although the high salinity conditions of 2% and 3% inhibited the anammox performance, it could be effectively recovered by dosing 5 g/L of SMB. The higher the influent salinity, the longer it took for SMB addition to restore its nitrogen removal performance. Consequently, a strategy to increase the dosage or frequency of SMB addition was implemented in reactors A_4 and A_5.

From Fig. 2c), after the first addition of 5 g/L of SMB in reactor A_4, the concentrations of NH_4^+-N, NO_2^--N, and TN in the effluent showed a slow decrease,

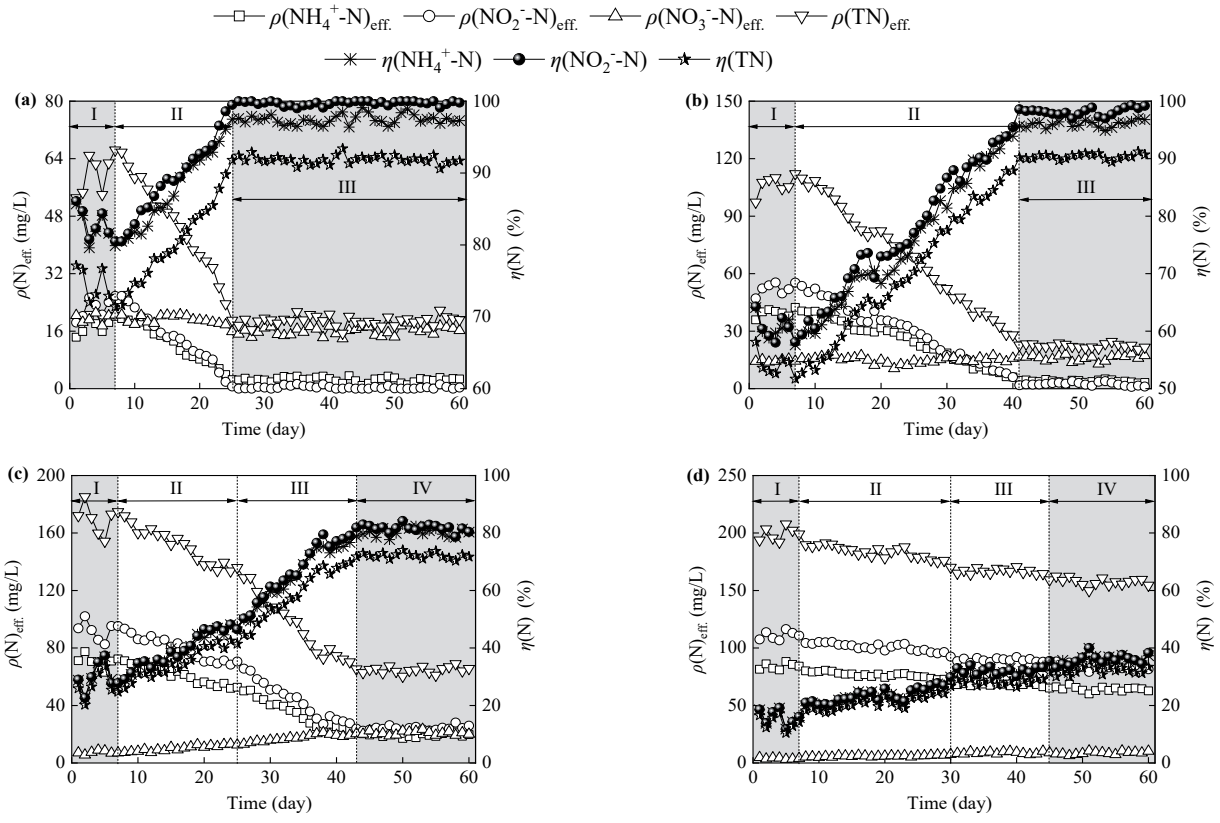

Fig. 2. Conversion of nitrogen pollutants in reactors a) A_2, b) A_3, c) A_4, and d) A_5 before and after SMB addition.

but the concentration of NO_3^--N increased slowly. The nitrogen removal efficiencies gradually recovered but were not as effective as those of reactors A_2 and A_3, and the value of η(TN) recovered only to about 40% after 18 days of operation in phase II, and then an additional 5 g/L of SMB was added to restore its nitrogen removal performance. At this time, the decreasing trend in nitrogen concentration in the effluent during phase III was observed to be enhanced, and the system entered the stabilized phase IV after 15 days of operation; the mean values of $\eta(NH_4^+\text{-N})$, $\eta(NO_2^-\text{-N})$, and η(TN) increased to 80.2%, 81.7%, and 72.1%, respectively, which were 50.3%, 51.7%, and 45.4% higher than those of phase I. Hence, the nitrogen removal effect of reactor A_4 was effectively improved by the addition of SMB twice, but the final recovery level was much lower than that of reactors A_2 and A_3. As shown in Fig. 2d), the nitrogen removal effect of reactor A_5 recovered only to a limited extent in phase II after the first addition of 10 g/L of SMB, and the value of η(TN) on the 29th day of operation only recovered to about 20%. At this time, another 5 g/L of SMB was added to enter phase III, and the nitrogen concentration in the effluent decreased at a slightly higher rate. The TN removal efficiency exceeded 30% on the 45th day of operation; thereafter, the change was no longer obvious, and the system entered phase IV. The average values of $\eta(NH_4^+\text{-N})$, $\eta(NO_2^-\text{-N})$, and η(TN) during phase IV were 35.6%, 36.0%, and 32.1%, respectively, which were only 19.8%, 20.1%, and 17.9% higher than those of phase I.

Consequently, after adding SMB, the VNRL values of reactors A_2 and A_3 gradually recovered to approximately 0.32 kgN/(m^3·d), approaching that of reactor A_0, which was unaffected by salinity suppression. In contrast, the VNRL values of reactors A_4 and A_5 during the stable period recovered only to about 0.25 and 0.11 kgN/(m^3·d), respectively, indicating an unsatisfactory recovery. Therefore, when the influent salinity ranged from 4% to 5%, increasing the SMB dosage or addition frequency could moderately enhance nitrogen removal, but the effectiveness diminished as influent salinity increased.

Variation of Stoichiometric Ratios

The anammox reaction holds specific stoichiometric ratios, and when the values of $\Delta NO_2^-\text{-N}/\Delta NH_4^+\text{-N}$ (α) and $\Delta NO_3^-\text{-N}/\Delta NH_4^+\text{-N}$ (β) are close to 1.32 and 0.26, respectively, this indicates that the main nitrogen loss pathway in the bioreactor is anammox [26]. However, multiple nitrogen removal pathways often occur simultaneously during actual operation, resulting in a discrepancy between the actual and theoretical stoichiometric ratios.

The variation of stoichiometric ratios of each ASBR before and after SMB addition is shown in Fig. 3. In Fig. 3a) and b), the mean values of α (β) for reactors A_2 and A_3 in phase I were 1.3284 (0.2386) and 1.3176 (0.2639), respectively, which were close to the theoretical stoichiometric ratios of the anammox reaction. Thus, the main nitrogen loss pathway within these ASBRs remained anammox when subjected to 2% and 3% salinity stress. After the addition of SMB, the values of stoichiometric ratios fluctuated significantly, indicating

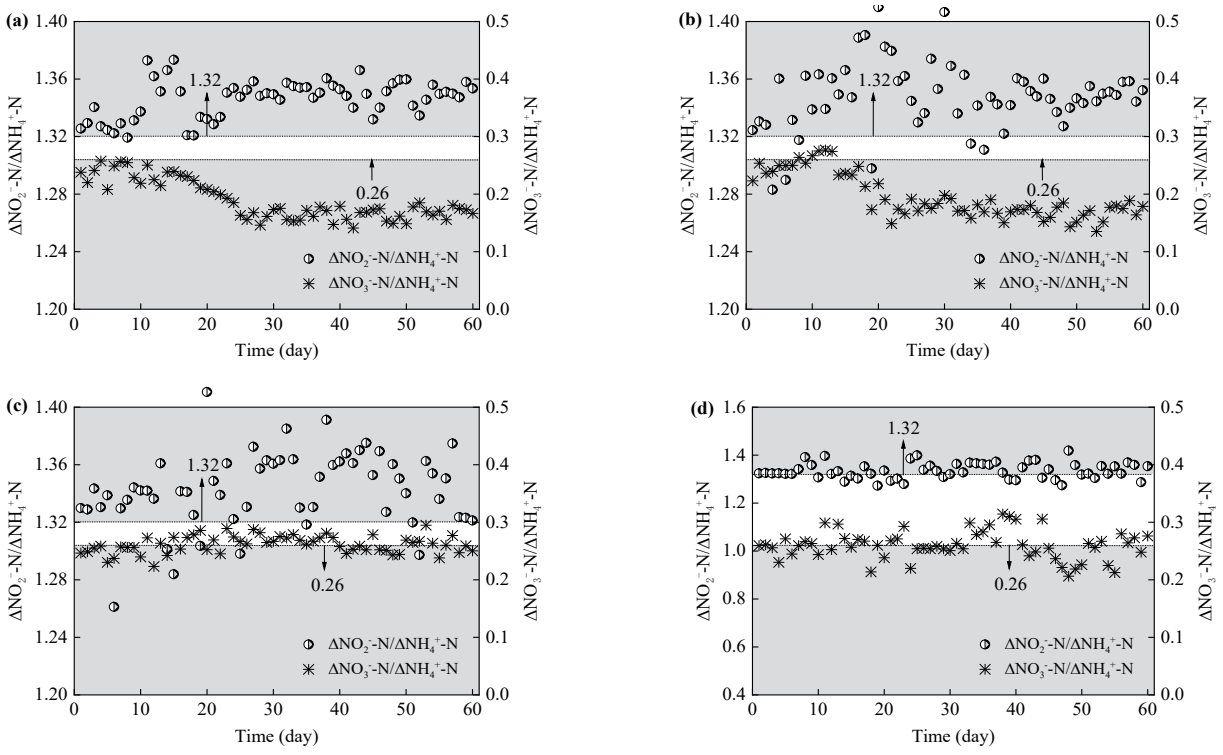

Fig. 3. Variation of stoichiometric ratios of reactors a) A_2, b) A_3, c) A_4, d) and A_5 before and after SMB addition.

the amplified influence of other pathways than anammox on the final nitrogen loss. After entering phase III, the mean values of α (β) in reactors A_2 and A_3 were 1.3508 (0.1646) and 1.3605 (0.1735), respectively, which began to deviate from the theoretical stoichiometric ratios of anammox. Comparison with phase I illustrated that the values of α increased, while the values of β decreased, which reflected that after the SMB injection, reactors A_2 and A_3 obtained higher NO_2^--N, NH_4^+-N, and NO_3^--N utilization rates, and the nitrogen loss pathways became more diversified. From Fig. 3c), the value of β for reactor A_4 in phase IV was close to 0.26, and the utilization of NO_3^--N was reduced. From Fig. 3d), the mean value of the stoichiometric ratio of reactor A_5 in phase IV was closer to the theoretical value of anammox, indicating that its main nitrogen loss pathway remained anammox. With the increase of influent salinity, the inducing effect of SMB addition on other nitrogen loss pathways weakened, and the subjectivity of the anammox reaction as the residual nitrogen loss pathway was enhanced, but its reactivity was also getting worse, and its nitrogen removal performance was seriously impaired and difficult to recover within a short period of time; thus, the mitigating effect of the salinity inhibition became more and more limited.

Variation of Nitrogen Removal Rate

To further resolve the effects of influent salinity and SMB dosing on the removal of NH_4^+-N and NO_2^--N, the experimental data were analyzed based on the proposed first-order kinetic model shown in Eq. (1), and the results are shown in Fig. 4.

$$\ln\frac{\rho(\mathrm{N})_{\mathrm{eff.}}}{\rho(\mathrm{N})_{\mathrm{inf.}}} = -kt + a \tag{1}$$

Where $\rho(N)_{inf.}$ and $\rho(N)_{eff.}$ denote the influent and effluent nitrogen concentrations (mg/L); t denotes time (h); k denotes the nitrogen removal rate constant (h^{-1}), and the larger value means the faster nitrogen removal [27]; a denotes the correlation constant.

From the analyzed results, reactor A_0 had high NH_4^+-N and NO_2^--N removal rates, with k values of 0.3497 and 0.4966 h^{-1}, respectively. When the influent salinity was increased to 2%~5%, a coercive effect caused by NaCl on the microorganisms appeared, and the anammox reaction was suppressed. With the increase of influent salinity, the k-value showed an obvious decreasing trend, especially when the influent salinity increased to 5%, the k-value corresponding to the removal of NH_4^+-N and NO_2^--N decreased to a very low level.

After the addition of SMB, nitrogen removal rates of the ASBRs inhibited by salinity were all elevated. The k values corresponding to NH_4^+-N and NO_2^--N removal in reactor A_2 were 1.96 and 2.66 times higher than those without SMB addition, which were close to reactor A_0, and thus, its nitrogen removal effect was better restored. The nitrogen removal rates of reactor A_3 were also similar to those of reactor A_0, and the nitrogen removal performance was basically restored to the original state. Nitrogen removal rates in reactors A_4 and A_5 rose above their phase I levels but remained low: 44.5% and 13.7% of the no-salinity shock for NH_4^+-N, and 34.3% and 9.6% of the no-salinity shock for NO_2^--N. The improvement in the rate of nitrogen removal by SMB diminished with increasing influent salinity.

Impact of Biochar on Sludge Properties

Changes in EPS Content

Fig. 5 reflects the changes in sludge EPS content before and after SMB addition. It can be seen that the EPS, PN, and PS contents in the sludge of reactor A_0 were 241.8, 194.7, and 47.1 mg/gVSS, respectively, corresponding to a value of 4.13 for PN/PS. EPS contains a large amount of extracellular polysaccharides, which can promote the adhesion between microorganisms and thus enhance the stability of granular sludge. A higher

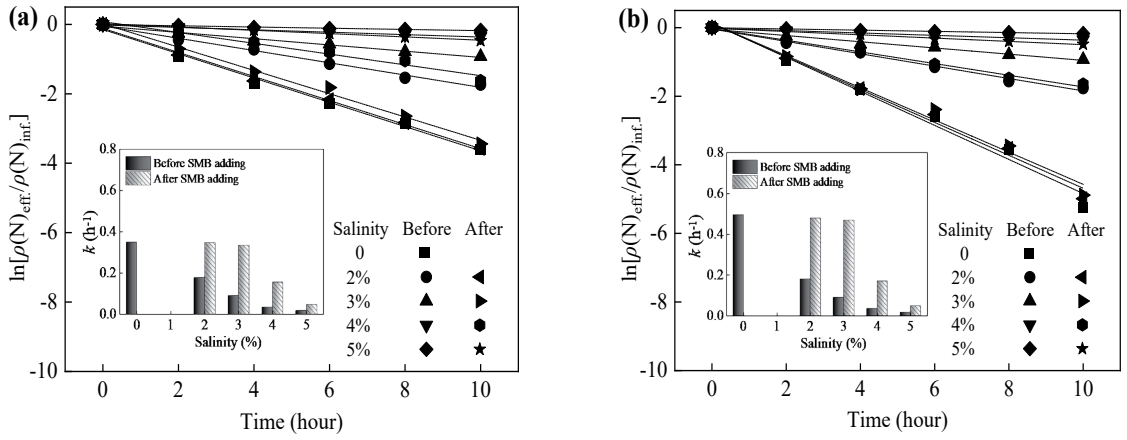

Fig. 4. Kinetic fitting results of a) NH_4^+-N and b) NO_2^--N removal in ASBRs before and after SMB addition.

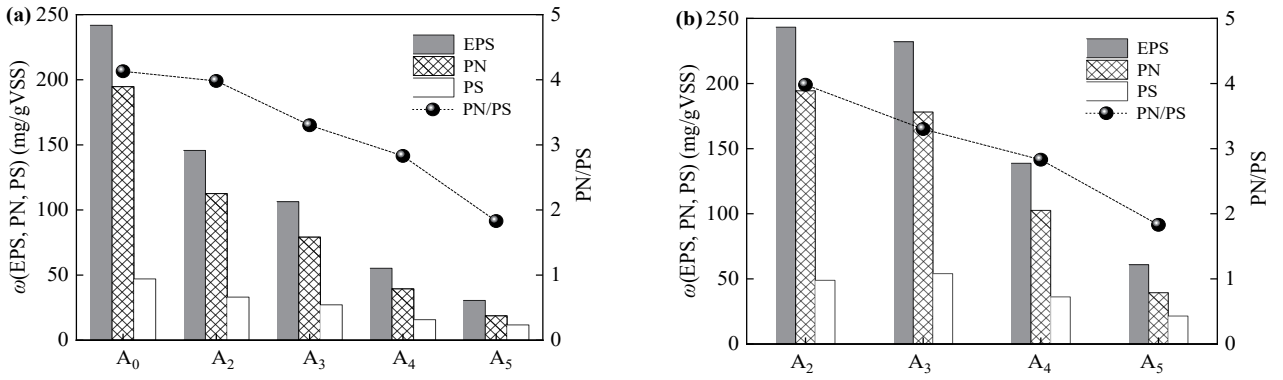

Fig. 5. Changes in sludge EPS content a) before and b) after SMB addition.

PN/PS value indicates greater granular sludge strength and hydrophobicity, which helps maintain the sludge in a granular state [28]. After salinity inhibition, the content of EPS, PN, and PS in sludge decreased, and the PN/PS ratio declined. As salinity increased, this downward trend gradually intensified. The degree of sludge granularity progressively decreased, microbial surface hydrophobicity deteriorated, interparticle aggregation weakened, affinity diminished, and sedimentation capacity declined.

After SMB addition and reaching the stable phase, the EPS, PN, and PS contents in the sludge of reactor A_2 (A_3) increased by 97.6 (125.7), 81.8 (98.9), and 15.8 (26.8) mg/gVSS, respectively, and the corresponding PN/PS ratio increased by 0.58 (0.39). This indicated that SMB addition effectively stimulated cells to produce more EPS, thereby promoting bacterial adhesion and enhancing resistance to salinity [29]. The EPS, PN, and PS contents in the sludge of reactor A_4 (A_5) also increased, but the increase was relatively small, with the corresponding PN/PS values only recovering to 2.83 (1.83). The remodeling ability of SMB on anammox granular sludge was best at 2% to 3% of influent salinity. The strengthening effect worsened with the increase of influent salinity, and the effluent concentration of TN increased. However, it was undeniable that when the influent salinity was 4%~5%, the appropriate increase of SMB could still promote the recovery of anammox granular sludge and have a positive effect on nitrogen removal.

Changes in Sludge SAA

The value of SAA in reactor A_0 was 1.386 kgN/(kgVSS·d), indicating that AnAOB within the sludge was of high activity [30]. When the influent salinity was 2%, 3%, 4%, and 5%, the values of SAA decreased to 1.071, 0.802, 0.406, and 0.219 kgN/(kgVSS·d), respectively, and the activity of AnAOB within the sludge was under increasingly heavy stress, while the nitrogen removal effect became increasingly poor. After SMB addition and stable operation, the SAA values of reactors A_2 and A_3 increased by 29.4% and 71.8%, respectively, compared with those before SMB addition, which were similar to the value of reactor A_0, indicating that the addition of SMB could effectively improve the metabolic activity of AnAOB, so that they still maintained a good nitrogen removal ability under high-salinity influent conditions. In reactor A_4, the SAA value of the sludge increased by 0.606 kgN/(kgVSS·d) after the addition of SMB compared with that before the addition, but it was far inferior to that of reactors A_2 and A_3. In reactor A_5, after the stabilization of the operation with SMB addition, the SAA value of sludge only recovered to 0.502 kgN/(kgVSS·d), suggesting that the strengthening effect of SMB addition on sludge activity was not enough to offset the negative impact of salinity on the system.

Structural Changes in SMB

SEM Characterization Results

The SEM characterization results of SMB before and after addition to ASBRs are shown in Fig. 6. Observations showed that the original SMB was distributed with a large number of holes of different sizes, uneven surface roughness, and a large holding space. After adding the SMB to reactors A_2 and A_3, the amount of pores decreased dramatically and the surface was covered with a layer of mud-like material, which indicated that the sludge could use the SMB as a carrier for microorganisms to attach and grow inside and outside of its pores to form a layer of biofilm structure when the influent salinity was 2% to 3% [31]. The higher surface coverage of SMB in reactor A_2 indicated that the microorganisms in the sludge could better attach to the SMB and form a more stable biofilm structure when subjected to a relatively low salinity shock. With increasing salinity, the coverage of sludge on the SMB surface in reactor A_3 decreased, and higher salinity would gradually be unfavorable to the growth of microbial attachment on the SMB. When the salinity reached 4%~5%, the remaining pore structure on the SMB gradually increased, which indicated that it was difficult for microorganisms to successfully

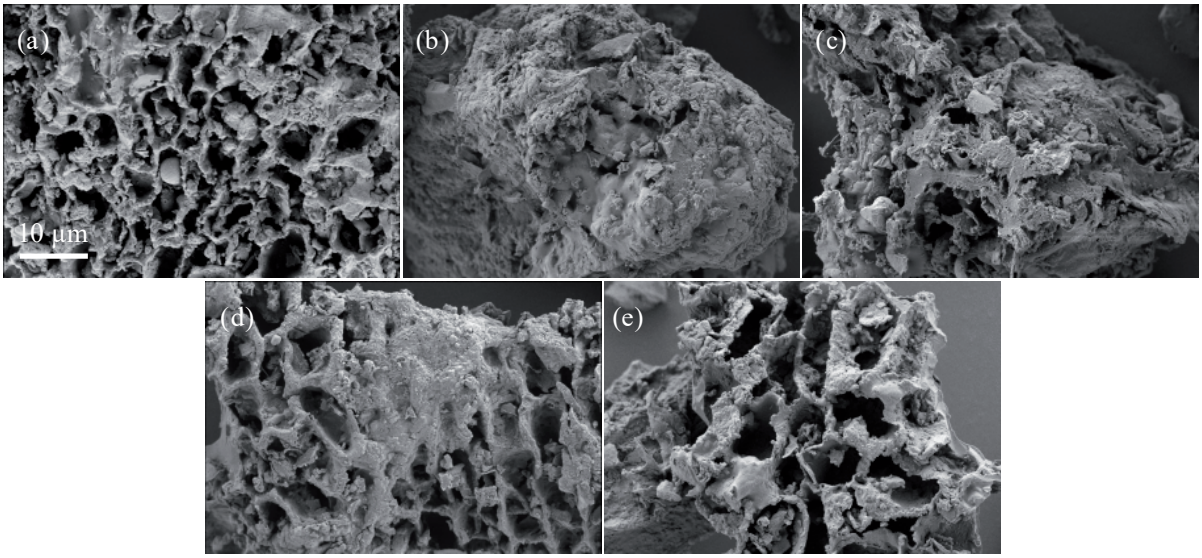

Fig. 6. Comparison of SEM photographs of a) original SMB and SMB after addition to reactors b) A_2, c) A_3, d) A_4, and e) A_5.

attach and form a stable biofilm structure on the SMB under relatively higher salinity conditions, and the higher the salinity, the greater this difficulty. In the range of higher influent salinity (4%~5%), the activity of microorganisms was severely inhibited, the secretion of mucilage was gradually reduced, and the ability to attach to the surface and interior of the SMB would become poorer, and thus the possibility of forming biofilm and its stability would be consequently reduced.

BET Characterization Results

The values of SSA, TPV, and ADP of the original SMB were 209.527 m^2/g, 0.291 cm^3/g, and 13.588 nm, respectively. Good pore structure cannot only provide excellent habitat for microbial attachment and growth on SMB, but also better adsorb nitrogen pollutants from wastewater to provide sufficient nutrients for microorganisms to grow better [32].

After addition to the ASBRs and stabilization, the values of SSA, TPV, and ADP of SMB-A_2 were 75.5%, 86.6%, and 80.2% lower than the original SMB, respectively. This indicated that the SMB interacted with the sludge in reactor A_2, resulting in a large number of microorganisms attached to the pores, which echoed the results of the SEM analysis. This attachment can promote the growth and metabolic activities of microorganisms and provide them with a "house" function to resist the adverse effects of NaCl, especially the microorganisms attached to the inner space of the SMB, which can better resist the salinity stress, thus enhancing the performance of sludge [33]. The decline in SSA, TPV, and ADP values for SMB-A_3 was slightly less than that for SMB-A_2, indicating that higher salinity shocks reduced microbial attachment to SMB and weakened their resistance to salinity inhibition. Comparison with the original SMB revealed that the values of SSA and TPV of SMB-A_4 (SMB-A_5) decreased by 28.6% (14%) and 35.7% (16.5%), respectively, while the value of ADP increased by 6.8% (14.7%). It was evident that the microorganisms could not fully recover their activity even with more SMB added when the influent salinity was 4% to 5%. The microorganisms occupied only a small portion of the tiny pores of the SMB, making it difficult to form a biofilm structure that could fully resist the impact of salinity, and thus, the recovery of the nitrogen removal performance of reactors A_4 and A_5 was limited.

FTIR Characterization Results

Fig. 7 reflects the FTIR analysis results of SMB before and after addition to the ASBRs. The analysis of raw SMB showed absorption peaks at 3424, 2971, 2925, 1621, 1316, 1048, 880, and 781 cm^{-1}, indicating that it was rich in functional groups such as –OH, C–H, C=C, C=O, and C–O. After the addition to reactors A_2 and A_3, the –OH, C=C, C=O, C–H, C–O stretching vibration peaks, and the C–H bending vibration peaks detected on the SMB exhibited varying degrees of shift, new appearance, or disappearance. In contrast, after the addition to reactors A_4 and A_5, only partial shifts or disappearances occurred. The change in the functional groups on the surface of the SMB implied that the pore structure, physical and chemical properties were changing, which in turn affected the nitrogen removal efficiency and recovery status of the anammox process.

Changes of functional groups critically affected biofilm formation and nitrogen removal performance under high-salinity conditions from multiple aspects. First, under high-salinity stress, –OH/C=O functional groups on SMB preferentially hydrated to form a localized hydration shield layer or reduced extracellular Na^+ concentration via ion exchange, alleviating the osmotic shock of Na^+ on the cell membrane. This accelerated biofilm maturation and rapidly restored

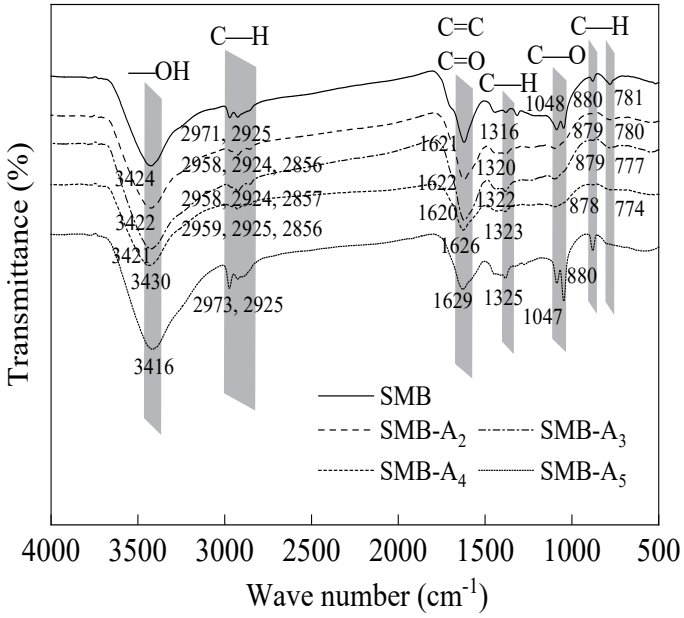

Fig. 7. FTIR analysis results of SMB before and after addition to the ASBRs.

anammox activity. Second, functional groups formed –CONH– bonds with $–NH_2$ groups in EPS, increasing the binding energy between biofilm and SMB. This directly promoted microbial colonization and accelerated biofilm thickness accumulation [34]. Additionally, functional groups such as –OH, C–H, and C–O on SMB possess good electron-donating ability, and functional groups such as C=O and C=C possess electron-accepting ability, and thus it also exhibits a high redox function, which can be used as an electron shuttle (ES) to mediate the extracellular electron transfer (EET) process [35]. Fu et al. showed that the addition of biochar increased the electron transfer activity of the anammox reaction system by 33.6%~41.9%, and it facilitated electron transfer by promoting the secretion of EPS or by directly acting as insoluble ES to provide additional electrons [36]. Yang et al. similarly demonstrated that the addition of biochar could stimulate the secretion of EPS, especially PN, to obtain higher electron transfer activity in the bioreactive system [37]. The results obtained in this study are consistent with the above studies. SMB not only promoted the secretion of EPS but also existed as an insoluble ES within the system to be cyclically oxidized and reduced, providing sufficient electron

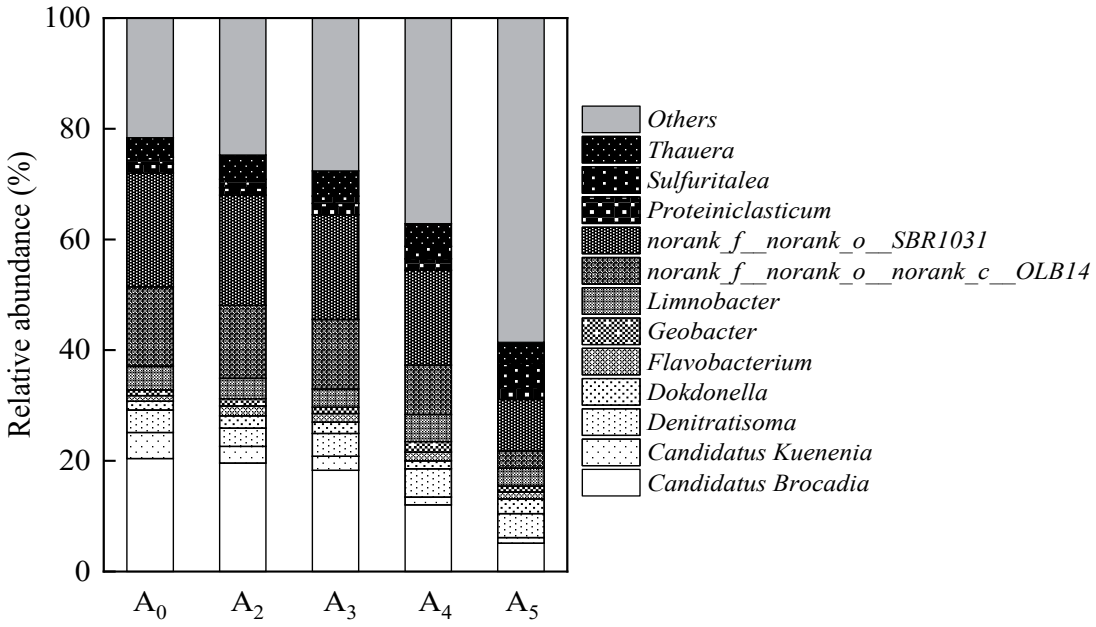

Fig. 8. Genus-level distribution of the microbial community.

donors and acceptors for the nitrogen removal process, facilitating electron transfer, or directly providing electrons to accelerate the metabolism of AnAOB, and thus improving the anammox performance under saline conditions. In summary, the reinforcing effect of SMB depended not only on its favorable pore structure but also on the dynamic evolution of its surface functional groups. However, the higher the salinity, the lower the involvement of functional groups in these processes and thus the less effective their enhanced nitrogen removal.

Structural Change in Microbial Community

Fig. 8 shows the genus-level distribution of the microbial community within reactor A_0 and reactors A_2~A_5 (after SMB addition). It can be observed that *Candidatus Brocadia* and *Candidatus Kuenenia*, as typical AnAOB genera [38], exhibited relative abundance sums of 25.13%, 22.62%, 20.82%, 13.44%, and 6.14% in reactors A_0, A_2, A_3, A_4, and A_5, respectively. *Norank_f_norank_o__norank_c_OLB1* and *norank_f_norank_o__SBR1031*, as typical filamentous fungal genera [39], exhibited relative abundances of 34.89%, 33.09%, 31.47%, 26.07%, and 12.41% in reactors A_0, A_2, A_3, A_4, and A_5, respectively. At influent salinities of 2%~3%, SMB addition maintained the abundance of these genera, preserving stable sludge structure and nitrogen removal efficiency. However, when influent salinity reached 4%~5%, their combined relative abundance declined significantly, leading to loose sludge structure and reduced nitrogen removal.

Additionally, *Denitratisoma* and *Limnobacter*, capable of heterotrophic denitrification, and *Thauera*, possessing nitrate reduction capabilities, were identified within the reactors [40, 41]. SMB addition mitigated the stress imposed by high salinity conditions on these species, effectively sustaining their relative abundances. *Denitratisoma* and *Limnobacter* could utilize organics produced by microbial metabolism or death in granular sludge as a carbon source for nitrogen transformation, contributing to nitrogen removal. *Thauera* could reduce NO_3^--N to NO_2^--N through short-path denitrification, providing more abundant substrates for anammox or denitrification reactions, thereby enhancing nitrogen removal efficiency.

Conclusions

With the increase in salinity in the wastewater, the nitrogen removal performance of the anammox process deteriorated. When inhibited by a salinity of 2%~3%, the addition of 5 g/L of SMB exhibited a positive effect on enhancing the nitrogen conversion efficiency, specific anammox activity, and maintaining bacterial structural stability, which resulted in the recovery of nitrogen removal. The higher the influent salinity, the longer it took to restore the nitrogen removal efficiency of the anammox process to a similar level via SMB addition. When the influent salinity was as high as 4%~5%, the anammox process was seriously inhibited, and increasing the frequency or dosage of SMB could not restore the nitrogen removal performance in a short period of time. The SMB-enhanced anammox process showed good feasibility when applied to nitrogen removal from wastewater with a salinity of 2% to 3%.

Acknowledgments

This study was financially supported by the Open Fund of Sichuan Provincial Engineering Research Center of Livestock Manure Treatment and Recycling (LMTR202505), the Open Fund of Engineering & Technology Center of Groundwater Pollution Control for Environmental Protection in Sichuan (2024-01) and the CDTU Laboratory Open Fund Program (2025CHSYSKF02).

Conflict of Interest

The authors declare no conflict of interest.

References

1. ADAMS M., ISSAKA E., CHEN C. Anammox-based technologies: A review of recent advances, mechanism, and bottlenecks. Journal of Environmental Sciences, **148**, 151, **2025**.
2. TRINH P.H., LEE H.S., NGUYEN V.T., PARK H.D. Contribution of the microbial community to operational stability in an anammox reactor: Neutral theory and functional redundancy perspectives. Bioresource Technology, **419**, 132029, **2024**.
3. HUANG Y., JIANG L., WU B., LIU J., LIU Y., XIE L., ZHOU M., DENG L., WANG W., WANG L. Effect of suspended solids from anaerobic digested wastewater on performance and microbial community of autotrophic nitrogen removal process. Journal of Cleaner Production, **450**, 141973, **2024**.
4. ZHU X., FANG L., XU F., SUN J., ZHANG X., CAI J. Deciphering effect of complex organics on Anammox-sulfide autotrophic denitrification coupling system for landfill leachate treatment. Bioresource Technology, **439**, 133388, **2025**.
5. PALAZON M.B., ALTAMIRANO G.J.M., LOPEZ G.J., MARTINEZ G.A., OSORIO F. Performance and microbiome of an anammox biofilter for treating secondary wastewater: Effect of organic matter, low-strength nitrogen, and temperature. Process Safety and Environmental Protection, **194**, 1409, **2025**.
6. HOU X., LI X., ZHU X., LI W., KAO C., PENG Y. Advanced nitrogen removal from municipal wastewater through partial nitrification-denitrification coupled with anammox in step-feed continuous system. Bioresource Technology, **391**, 129967, **2024**.
7. HE Z., FAN G., XU Z., WU S., XIE J., QIANG W., XU K. A comprehensive review of antibiotics stress on anammox

systems: Mechanisms, applications, and challenges. Bioresource Technology, **418**, 131950, **2025**.
8. CHEN S., LIU C., CAO G., LI K., HUANG J. Effect of salinity on biological nitrogen removal from wastewater and its mechanism. Environmental Science and Pollution Research, **31** (17), 24713, **2024**.
9. GAO Z., WANG Y., CHEN H., LV Y. Biological nitrogen removal characteristics and mechanisms of a novel salt-tolerant strain *Vibrio* sp. LV-Q1 and its application capacity for high-salinity nitrogen-containing wastewater treatment. Journal of Water Process Engineering, **59**, 105098, **2024**.
10. MIAO Q., XIE Y., ISMAIL S., WANG Z.B., NI S.Q. Salt-tolerant marine sludge is more suitable for stable and efficient high-salinity wastewater treatment than activated sludge. Chemical Engineering Journal, **505**, 159404, **2025**.
11. QU Y., ZHAI Y., MA C., SHI W., ZHAO M., HUANG Z., RUAN W. Rapid start-up of anaerobic digestion reactor with rice-straw ash addition for treating high salinity organic wastewater. Process Safety and Environmental Protection, **175**, 806, **2023**.
12. CHEN L., ZHOU L., DING Y., WU D., FENG H. Enhancing microbial salt tolerance through low-voltage stimulation for improved p-chloronitrobenzene (p-CNB) removal in high-salinity wastewater. Science of the Total Environment, **905**, 167164, **2023**.
13. ZHU Y., HUO Y., ZHANG M., LI Z., HUANG Y. Study on the synergistic mechanism of proline in the treatment of high-salt phenolic wastewater by short-time aerobic digestion process. Environmental Monitoring and Assessment, **197** (1), 90, **2024**.
14. OKABE S., KAMIZONO A., KAWASAKI S., KOBAYASHI K., OSHIKI M. Interspecific competition and adaptation of anammox bacteria at different salinities: Experimental validation of the Monod growth model with salinity inhibition. Water Research, **271**, 122883, **2025**.
15. ZHANG Y., ZHANG X., ZHOU Z., LIU G., WANG C. A review of the conversion of wood biomass into high-performance bulk biochar: Pretreatment, modification, characterization, and wastewater application. Separation and Purification Technology, **361**, 131448, **2025**.
16. QIN Y., WEI Q., CHEN R., JIANG Z., QIU Y., JIANG Y., LI L. Roles of red mud-based biochar carriers in the recovery of anammox activity: characteristics and mechanisms. Environmental Science and Pollution Research, **31** (13), 20488, **2024**.
17. YANG B., WANG H., YAN Y., BAO P., FENG Q., CHEN B., JIA Y., SHU W., LU H. Coupling microalgae-based biochar with MBGS enhances microbial synergy and multi-pollutant removal from saline aquaculture wastewater. Water Research, **289**, 124881, **2026**.
18. ZHAO L., FU G., PANG W., TANG J., GUO Z., HU Z. Biochar immobilized bacteria enhances nitrogen removal capability of tidal flow constructed wetlands. Science of the Total Environment, **836**, 155728, **2022**.
19. WANG Z., GU Z., YANG Y., DAI B., XIA S. Review of biochar as a novel carrier for anammox process: Material, performance and mechanisms. Journal of Water Process Engineering, **50**, 103277, **2022**.
20. LU Y., CHEN J., BAI Y., GAO J., PENG M. Adsorption properties of methyl orange in water by sheep manure biochar. Polish Journal of Environmental Studies, **28** (5), 3791, **2019**.
21. WANG S., LI X., ZHU Y. Comparison of the adsorption capacity and mechanisms of mixed heavy metals in wastewater by sheep manure biochar and Robinia pseudoacacia biochar. Water Science and Technology, **87** (12), 3083, **2023**.
22. CHEN J., LU Y., HUANG W., WU J., LI B., ZHANG J. Effect of organic matter on the anammox performance of constructed rapid infiltration systems. Environmental Technology, **43** (12), 1770, **2022**.
23. LU Y., LIU Y., LI C., LIU H., LIU H., TANG Y., TANG C., WANG A., WANG C. Adsorption characteristics and mechanism of methylene blue in water by NaOH-modified areca residue biochar. Processes, **10** (12), 2729, **2022**.
24. XIONG T.Y., LIAO W.X., GUO S.J., FANG F., CHEN P.Y., YAN P. Potential role of the anammoxosome in the adaptation of anammox bacteria to salinity stress. Environmental Science & Technology, **58** (15), 6670, **2024**.
25. WANG M., CHEN S., GAO M., ZHAO Y., JI J., ZHANG Z., ZHU L., XU X. Rethinking the effect of salinity on nitrogen removal capacity of aerobic granular sludge from the perspective of size distribution and granular morphology. Environmental Research, **266**, 120580, **2024**.
26. TANG B., WANG J., GAO X., LI Z. Strategies for efficient enrichment of anaerobic ammonia oxidizing bacteria in activated sludge. Journal of Environmental Sciences, **151**, 703, **2025**.
27. AKA N.J.R., HOSSAIN M.M., NASIR A., ZHAN Y., ZHANG X., ZHU J., WANG Z.W., WU S. Enhanced nutrient recovery from anaerobically digested poultry wastewater through struvite precipitation by organic acid pre-treatment and seeding in a bubble column electrolytic reactor. Water Research, **252**, 121239, **2024**.
28. KAN X., JI B., ZHANG J., LIU Z., XU Y., ZHAO L., SHI B., PU J., ZHANG Z. Advances in aerobic granular sludge stabilization in wastewater. Desalination and Water Treatment, **319**, 100513, **2024**.
29. QIAN J., LUO D., YU P., YE B., LI Y., WANG Y., GAO Y., FU J. Insights into the reaction of anammox to exogenous pyridine: Long-term performance and micro mechanisms. Bioresource Technology, **384**, 129273, **2023**.
30. WANG W., WANG L., WANG Q., SU Y., LI J., LI D. The start-up of red blood cell-like Anammox granular sludge based on substrate volume flux. Process Biochemistry, **149**, 121, **2025**.
31. ZHONG H., JIANG C., HE X., HE J., ZHAO Y., CHEN Y., HUANG L. Simultaneous change of microworld and biofilm formation in constructed wetlands filled with biochar. Journal of Environmental Management, **349**, 119583, **2024**.
32. YANG B., SUN J., WANG Z., DUAN Y. Sustainable biochar application in anammox process: Unveiling novel pathways for enhanced nitrogen removal and efficient start-up at low temperature. Bioresource Technology, **402**, 130773, **2024**.
33. DORNER M., BEHRENS S. Biochar as ammonia exchange biofilm carrier for enhanced aerobic nitrification in activated sludge. Bioresource Technology, **413**, 131374, **2024**.
34. MA J., HU L., YAO J., WANG Z., LI A., HRYNSPHAN D., SAVITSKAYA T., CHEN J. A novel macroporous biochar as a biocarrier for DMAC biodegradation: Preparation, performance and mechanism. Journal of Environmental Chemical Engineering, **12** (2), 112038, **2024**.
35. LV L., JIA C., WEI H., ZHAO P., CHEN R. Biochar modulates intracellular electron transfer for nitrate reduction in denitrifying anaerobic methane oxidizing archaea. Bioresource Technology, **406**, 130998, **2024**.

36. FU J., LI Q., DZAKPASU M., HE Y., ZHOU P., CHEN R., LI Y.Y. Biochar's role to achieve multi-pathway nitrogen removal in anammox systems: Insights from electron donation and selective microbial enrichment. Chemical Engineering Journal, **482**, 148824, **2024**.
37. YANG W., XIN X., LIU S. Performances of a novel BAF with ferromanganese oxide modified biochar (FMBC) as the carriers for treating antibiotics, nitrogen and phosphorus in aquaculture wastewater. Bioprocess and Biosystems Engineering, **47** (11), 1849, **2024**.
38. ZHANG H., ZHANG J., HU X. Analyzing the nitrogen removal performance and cold adaptation mechanism of immobilized cold-acclimation ANAMMOX granules at low temperatures. Water Environment Research, **96** (2), 10985, **2024**.
39. ZHANG H., ZHANG X., MA Y., SONG Y., WANG Q., ZHANG K., MA B. Synergistic removal of total nitrogen and bisphenol A through MBR-Anammox system. Journal of Environmental Chemical Engineering, **13** (4), 117376, **2025**.
40. DENG Z., CHEN Y., ZHANG C., CHEN Z., LI Y., HUANG L., WANG Z., WANG X. Improving nitrogen removal performance from rare earth wastewater via partial denitrification and anammox process with Fe(II) amendment. Journal of Water Process Engineering, **60**, 105131, **2024**.
41. TANG L., GAO M., LIANG S., WANG S., WANG X. Enhanced biological phosphorus removal sustained by aeration-free filamentous microalgal-bacterial granular sludge. Water Research, **253**, 121315, **2024**.